



The influence of sea currents on the behaviour of the *SWAN* model in the Diogo Lopes area, Brazil

André Filipe Santos Ramos

andre.ramos@ist.utl.pt

Department of Civil Engineering, Architecture and Georesources, Instituto Superior Técnico, ULisboa, Av. Rovisco Pais, 1049-001, Lisbon-Portugal

July 2014

Abstract : Over the past few years the Diogo Lopes region, located in the state of Rio Grande do Norte, Northeast Brazil, has been the object of a number of interdisciplinary studies including the characterization of its wave climate (Ângelo, 2012; Matos, 2013). The wave climate is characterized by a breeze regime. The alternation between the sea and land breezes along this coastline posed a few difficulties to its correct modelling. In order to overcome these difficulties, the *SWAN* model was used once again to simulate the wave propagation. This time a larger domain and a different wind field, obtained in the meteorological station in Macau (RN), were employed. Also, a current field was imposed to take into account wave-currents interaction. These currents were calculated by the hydrodynamic model *SISBAHIA*, developed in the Federal University of Rio de Janeiro (UFRJ). The offshore wave conditions were obtained from the deep-water wave model, *Wavewatch III* (Tolman, 2002). Field data were obtained through the measurements of *AWAC* sensors for the time periods from the 11th to the 12th of December 2010 and from the 20th to the 27th December 2010 in two distinct points inside the computational grid. The analysis of the results was accomplished resorting to both graphical analysis and statistic characterization.

Key words: *SWAN*; Wave-Currents; Diogo Lopes; *SISBAHIA*; Wave Climate; Whitecapping.

1 INTRODUCTION

The Diogo Lopes area, located in the state of Rio Grande do Norte, Northeast Brazil (Figure 1.1), is characterized by a tropical climate, which dominates the environment. In the study area there are minor estuaries of rivers and lagoons that desembogue in the Atlantic. Due to its complexity, this area has been the focus of several environmental studies and monitoring programs, which intend to contribute to the understanding of the coastal processes and their evolution. In those studies Matos (2013), among others, have pointed out to the need of better knowledge on waves, tides and winds, as well on the hydrodynamic circulation in the study area. In fact, the complex bathymetry and tidal circulation make the wave propagation not a trivial exercise and the correct estimation of the wave field here is of paramount importance for sediment dynamics, coastal morphodynamic

studies, and coastal engineering design. Furthermore, the wave climate in Diogo Lopes is mainly affected by the alternation between the sea and land breezes. However, existing information regarding sea waves and their propagation in this region are insufficient for any study of coastal engineering. To overcome this problem, numerical models of wave propagation constitute a viable alternative for estimating the wave climate. In the present study, the *SWAN* model, that stands for *Simulating WAVes Nearshore* (Booij et al., 1999), was used to simulate the sea state. This model estimates the characteristic parameters of the wave climate through the directional spectrum. More specifically, the present dissertation follows the work developed by Ângelo (2012) and Matos (2013) that applied the *SWAN* model with different wind and offshore conditions, comparing the numeric simulations with measurements *in situ* in two distinct points (PT1 and PT2) for the time periods from the 11th to the 12th of December 2010 and from the 20th to the 27th December 2010.

Figure 1.1 - Diogo Lopes location in the state of Rio Grande do Norte, Brazil. Adapted Google Maps.



The results obtained through these studies were quite satisfactory. However, some differences were noticed between the calculated and the observed values of the mean period (T_{m02}). One of the major suggestions made by the authors of these works, to improve the calculated values of the mean period, was to include a current field in the *SWAN* model simulations. In fact, since the study area is located in an estuary zone, this wave-current interaction becomes of major importance. With a current field is possible to consider the Doppler effect and consequently it is expected that the calculated values of the mean wave period become closer to the real ones. The present dissertation consisted in the application of the *SWAN* model in the Diogo Lopes area forced in the offshore boundary and by a wind field. Moreover, the wave field will be propagated in a current field within the *SWAN* computational grid. The former was substantially extended in the seaward direction. The *SWAN* model is applied to the time periods from the 11th to the 12th and from the 20th to the 27th of December 2010. The numeric results are compared with the field measurements obtained in these same time periods.

2 THE SWAN MODEL

The *SWAN* model (Booij et al., 1999; SWAN Team, 2008) is a third generation spectral wave model designed to simulate wave propagation in a large range of depths, including nearshore shallow waters. In order to operate this

model, the user has to define a computational grid, associated to a bathymetry grid. The model uses implicit numerical schemes. The offshore boundary conditions result from the coupling with deep water oceanic scale models like *WAM* or *Wavewatch III*.

The *SWAN* model is based on the spectral action balance equation. This equation may be formulated in spherical coordinates for big scale computations or Cartesian coordinates for smaller applications. In the present dissertation, the equation (2.1) was used in Cartesian coordinates.

$$\frac{\partial N(\sigma, \theta; x, y, t)}{\partial t} + \frac{\partial c_{gx} N(\sigma, \theta; x, y, t)}{\partial x} + \frac{\partial c_{gy} N(\sigma, \theta; x, y, t)}{\partial y} + \frac{\partial c_{\theta} N(\sigma, \theta; x, y, t)}{\partial \theta} + \frac{\partial c_{\sigma} N(\sigma, \theta; x, y, t)}{\partial \sigma} = \frac{S(\sigma, \theta; x, y, t)}{\sigma} \quad (2.1)$$

This equation uses the action density $N(\vec{x}, t, \sigma, \theta)$ in space \vec{x} and time t , instead of the spectral energy density E , since E is not conservative when propagating between waves and currents.

$$N(\sigma, \theta) = \frac{E(\sigma, \theta)}{\sigma} \quad (2.2)$$

σ represents the relative frequency and θ is the wave direction.

The left member of (2.1) represents the local variation and the cinematic component of the propagation in its various dimensions. The right member represents the source and sinks terms. The second and third parcels, of the left member, correspond to the wave propagation in the geographic space with propagation velocities $c_{g,x}$ and $c_{g,y}$ in x and y space, respectively. The fourth parcel includes in this equation the refraction induced by the depth variation and trough the currents effect, with c_{θ} corresponding to the spectral space velocity, θ (wave direction). Finally, the fifth parcel stands for the variation of the angular frequency due to variations of the depth and currents, with c_{σ} corresponding to the propagation velocity in the relative frequency domain, σ .

The left term of (2.1), $S(\sigma, \theta)$, stands for the effects of generation by wind $S_{in}(\sigma, \theta)$, non-linear wave-wave interactions $S_{nl}(\sigma, \theta)$ and dissipation $S_{diss}(\sigma, \theta)$.

3 CASE STUDY – THE DIOGO LOPES ESTUARY, BRAZIL

3.1 The available data

As mentioned before, the present study had the objective of improving the application conditions of the *SWAN* model in this region, taking into account its climate characteristics and also the available data. In particular, the wind measurements were obtained at the Macau meteorological station at a 4 m height, the measurements of wave height, period and direction were made through two acoustic wave and current meter sensors (*AWAC*). The location of the sensors is represented in Figure 3.1. The wind field was considered constant in the whole domain, and was measured with a temporal resolution of one hour in the mentioned periods. The offshore boundary conditions, parameterized by the significant height H_s , peak period T_p and mean direction Dir , were obtained as the output of the *WAVEWATCH III* deep water model in one point. This point corresponds to the Cartesian coordinates UTM (787166.43 m, 9668067.83 m). The current field was obtained by the *SISBAHIA* model (*Sistema de Base Hidrodinâmica Ambiental*) (Rosman, 2000), and uses the *Large Eddy Simulation (LES)* as the turbulence closure model. The *SISBAHIA* model has been implemented and improved since 1987. This model is subdivided in multiple modules. For further information referring to *SISBAHIA* see Rosman (2000).

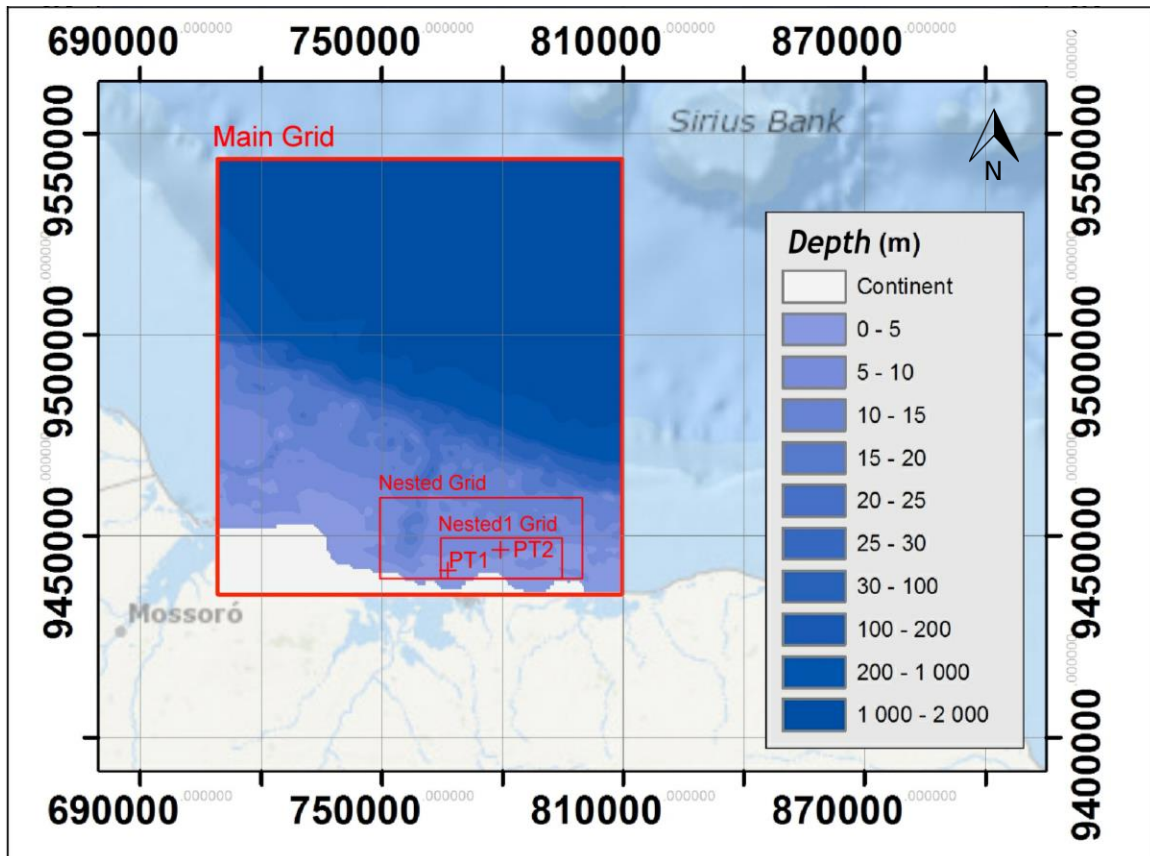


Figure 3.1 – Location of the Domain, nested grids and measurement points.

3.2 The SWAN model application conditions

The definition of the main SWAN grid was conditioned by the available bathymetry data in the Diogo Lopes area. The bathymetry used in the present dissertation is, essentially, the same used by Ângelo (2012) and Matos (2013). However, the seaward boundary was positioned further way with two main objectives. The previous main grid had a minor stretch that was located over medium shallow waters and this new one configures a domain totally over deep waters. On the other hand, it was possible to make the boundary closer to the *WWIII* output point. The SWAN grids properties can be consulted on Table 3.1.

The SWAN 40.72 version was used in this work. Diffraction, non-linear three and four wave interaction were some of the physical phenomena considered. Concerning the bottom friction the semi-empiric JONSWAP expression was adopted (Hasselmann et al., 1973). Depth induced breaking and whitecapping were also considered. The former was parameterized according to the van der Westhuysen et al. (2007) formulation for this phenomenon. The discretization of the directional spectra was made with 23 frequency intervals, between 0.04 Hz and 1.0 Hz, with a logarithmic distribution. Two operation modes – stationary and non-stationary were considered. Changes in the bottom friction coefficient to use in the JONSWAP formulation were experimented. However, simulations with a current field was the main test objective. In Ângelo (2012) a large number of bottom friction coefficients were tested. In the present work, this choice was narrowed to a couple of values. One of those values is the default value defined by the SWAN model for wind sea ($c=0.067 \text{ m}^2\text{s}^{-3}$) and the other was fixed in $c=0.1 \text{ m}^2\text{s}^{-3}$.

Summarizing, there were made 16 numerical simulations – 8 for each period of measurements. The entire bottom friction coefficient – currents conditions possible combinations were tested, as illustrated in Tables 3.2 and 3.3.

Table 3.1 - SWAN grids properties.

Grids	Origin (x, y) (m)	Dimensions(km)	$\Delta x(m)$	$\Delta y(m)$
Main Grid	(709869, 943260)	99.5x107.5	1000	1000
Nested grid	(750000, 9440000)	50x20	500	250
Inner grid (Nested1)	(765000, 9440000)	30x10	100	50

Table 3.2 - Numeric simulations conditions for the period from de 11th to the 12th of December 2010.

	Mode	Bottom Friction Coefficient (m^2s^{-3})	Currents' conditions
Simulation 1	Stationary	0.1	Yes
Simulation 2		0.1	No
Simulation 3		0.067	Yes
Simulation 4		0.067	No
Simulation 5	Non-stationary	0.1	Yes
Simulation 6		0.1	No
Simulation 7		0.067	Yes
Simulation 8		0.067	No

Table 3.3 - Numeric simulations conditions for the period from the 20th to the 27th of December 2010.

	Mode	Bottom Friction Coefficient (m^2s^{-3})	Currents' conditions
Simulation 9	Stationary	0.1	Yes
Simulation 10		0.1	No
Simulation 11		0.067	Yes
Simulation 12		0.067	No
Simulation 13	Non-stationary	0.1	Yes
Simulation 14		0.1	No
Simulation 15		0.067	Yes
Simulation 16		0.067	No

4 RESULTS: COMPARISON AND ANALYSIS

For all the graphics presented in this section, the same nomenclature was used in the definition of the numerical simulations, as follows:

“*Corr*” – Simulation which took into account a current field;

“*SemCorr*” – Simulation which did not take into account a current field;

“01” – Use of the $0.1 \text{ m}^2\text{s}^{-3}$ value for the bottom friction coefficient;

“0067” – Use of the $0.067 \text{ m}^2\text{s}^{-3}$ value for the bottom friction coefficient.

“Medições” – Measurements obtained *in situ*.

4.1 The 11th to 12th of December 2010 period

In this period, and in what concerns the significant wave height, the introduction of a current field did not induce major changes in this parameter. On the other hand, the bottom friction coefficient has an important role on the accuracy of the significant height’s behaviour. As expected, the increase of the bottom friction is accompanied by a decrease of the calculated significant height. It is possible to verify this in Figure 4.1, for PT1, and Figure 4.2 for PT2. In this period, the best-obtained values are accomplished when applying a $c=0.067 \text{ m}^2\text{s}^{-3}$ bottom coefficient value with a current field and in stationary mode.

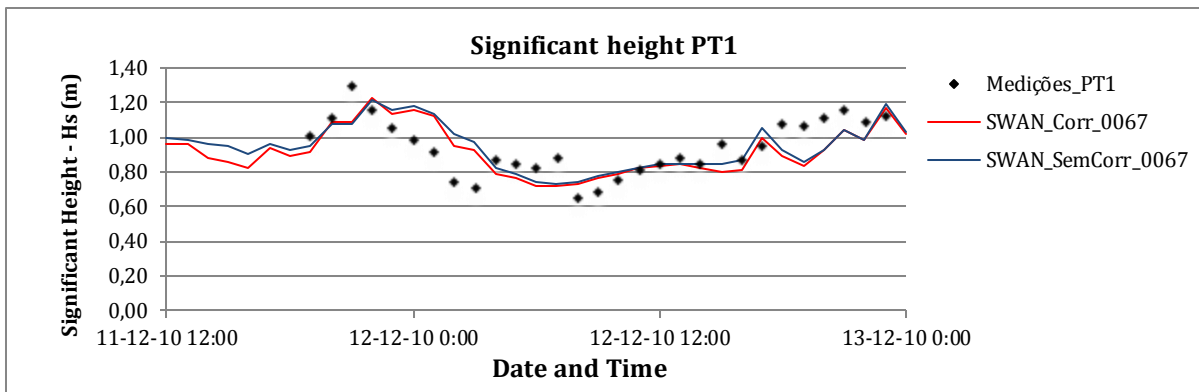


Figure 4.1 - Simulations 3 and 4. Significant height for PT1 from the 11th to the 12th December 2010. Stationary mode. $c=0.067 \text{ m}^2\text{s}^{-3}$.

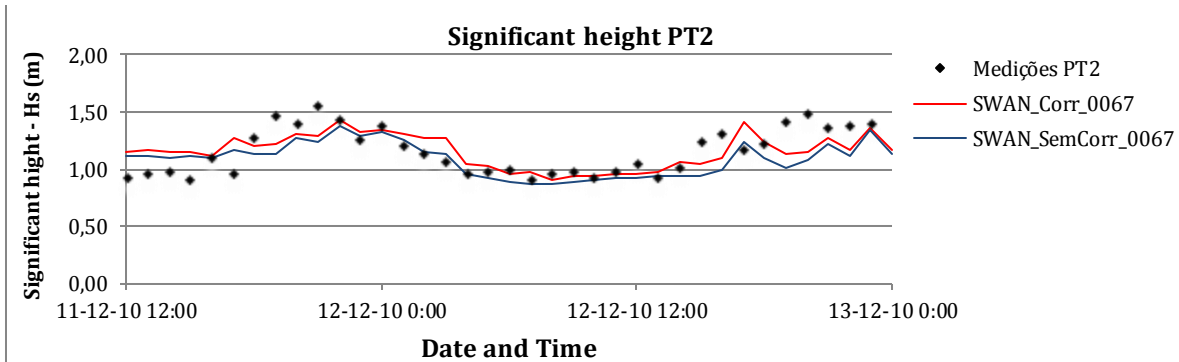


Figure 4.2 - Simulations 3 and 4. Significant height for PT1 from the 11th to the 12th December 2010. Stationary mode. $c=0.067 \text{ m}^2\text{s}^{-3}$.

Focusing now on the mean wave period, it is verified, in general, that it is possible to achieve improvements when considering a current field (Figures 4.3 and 4.4). However, the bottom friction coefficient’s values have also an important influence in the T_{m02} calculated values. The increase of the bottom friction coefficient’s values generates smaller values of the calculated T_{m02} .

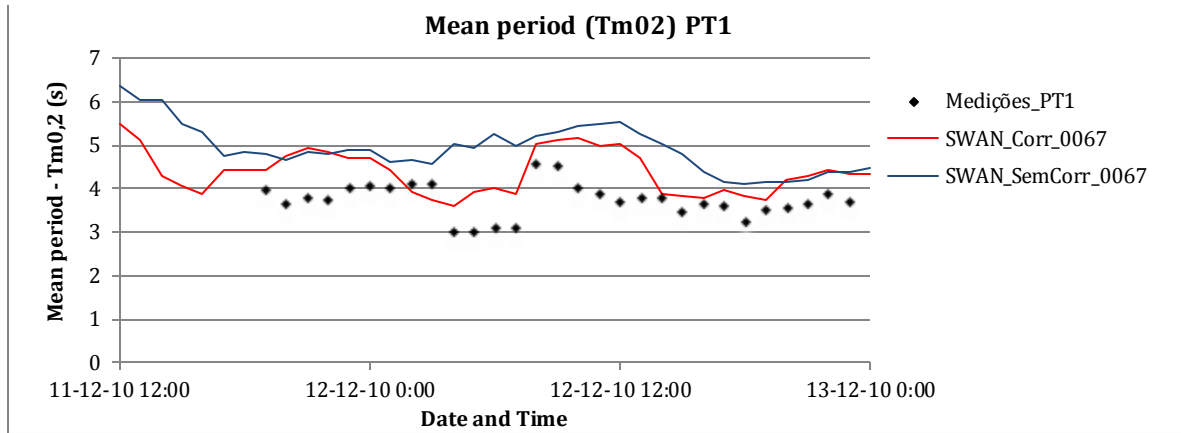


Figure 4.3 - Simulations 3 and 4. Mean period for PT1 from the 11th to the 12th December 2010. Stationary mode. $c=0.067 \text{ m}^2 \text{ s}^{-3}$.

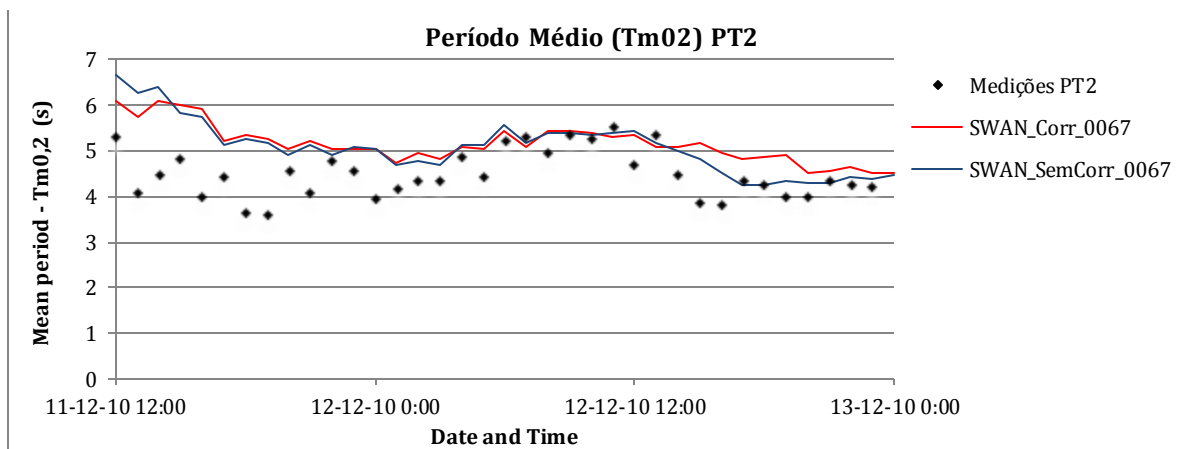


Figure 4.4 - Simulations 3 and 4. Mean period for PT2 from the 11th to the 12th December 2010. Stationary mode. $c=0.067 \text{ m}^2 \text{ s}^{-3}$.

For a better analysis the statistical parameters for simulations 3 and 4 are presented in Table 4.1.

Table 4.1 - Statistic parameters for the period from the 11th to the 12th December 2010 in stationary mode. ($c=0.067 \text{ m}^2 \text{ s}^{-3}$)

		Stationary mode					
$c(\text{m}^2 \text{ s}^{-3})$	Currents' conditions	PT1			PT2		
0.067	With currents (Simulation 3)	RMSE			RMSE		
		Hs(m)	Tm0,2(s)	Dir(°)	Hs(m)	Tm0,2(s)	Dir(°)
		0.127	0.732	23.097	0.204	0.961	67.044
		SI			SI		
		Hs	Tm0,2	Dir	Hs	Tm0,2	Dir
		0.134	0.196	---	0.177	0.211	---
	ME			ME			
	Hs(m)	Tm0,2(s)	Dir(°)	Hs(m)	Tm0,2(s)	Dir(°)	
	-0.021	0.616	-21.439	-0.226	-0.584	-15.468	
	Without currents (Simulation 4)	RMSE			RMSE		
		Hs(m)	Tm0,2(s)	Dir	Hs(m)	Tm0,2(s)	Dir
		0.130	1.164	25.209	0.228	0.965	66.509
SI			SI				
Hs		Tm0,2	Dir	Hs	Tm0,2	Dir	
0.138		0.311	---	0.199	0.212	---	
ME			ME				
Hs	Tm0,2	Dir	Hs	Tm0,2	Dir		
-0.002	1.046	-24.163	-0.280	-0.645	-14.596		

4.2 The 20th to 27th of December 2010 period

For the time period from the 20th to the 27th December 2010 it was possible to observe again that $c=0.067 \text{ m}^2\text{s}^{-3}$ corresponds to the best fit of the significant wave height. By the end of the period, the 26th and the 27th December 2010, there was a swell event. Eventually, for this specific period it would be better to use a different value for the friction coefficient, in particular, the one suggested in the JONSWAP experiments for swell conditions – $c=0.038 \text{ m}^2\text{s}^{-3}$. For more detailed information on this specific matter, see Ângelo (2012). It is also observable that the inclusion of the current field did not bring major changes in the simulated H_s (Figure 4.5). Once more, for this time period, the best results were obtained in stationary mode considering the bottom friction coefficient $c=0.067 \text{ m}^2\text{s}^{-3}$.

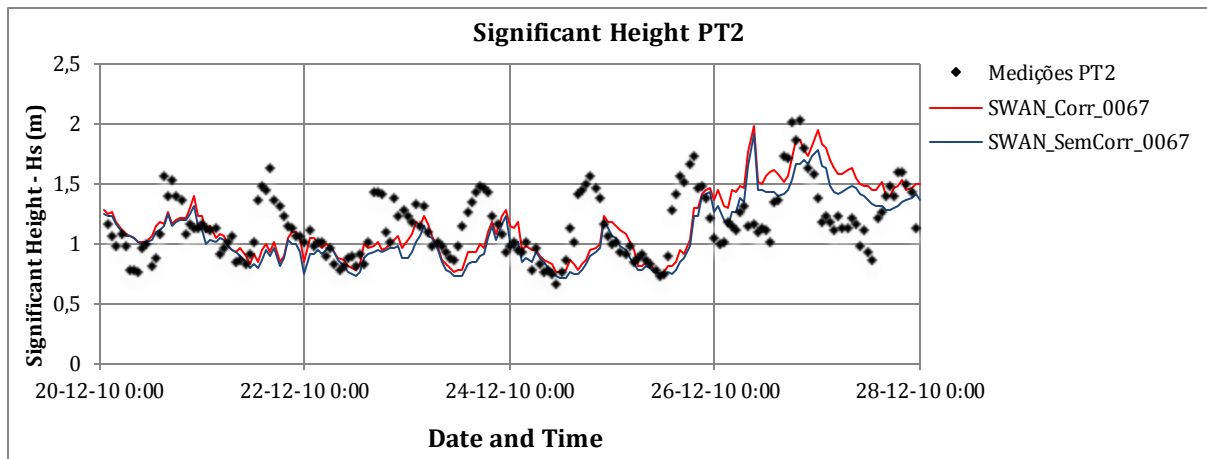


Figure 4.5 - Simulations 11 and 12. Significant height for PT2 from the 20th to the 27th December 2010. Stationary mode. $c=0.067 \text{ m}^2\text{s}^{-3}$.

As it is possible to observe in Figure 4.6, the simulations of the mean period (T_{m02}) exhibit a good adjustment to the *in situ* measurements, with the exception of the swell episode already mentioned. Concerning the currents' field consideration makes it possible to observe, in this specific case, that its inclusion in the simulations increases the T_{m02} calculated values. This way, the calculated values get closer to the *in situ* measurements.

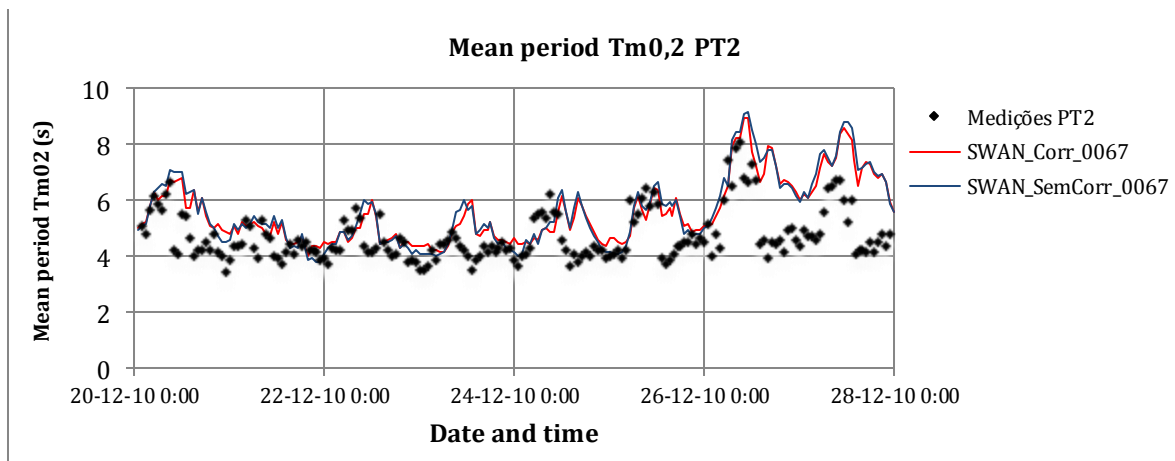


Figure 4.6 - Simulations 11 and 12. Mean period for PT2 from the 20th to the 27th December 2010. Stationary mode. $c=0.067 \text{ m}^2\text{s}^{-3}$.

For a better understanding of the observations mentioned above statistical parameters are presented in Table 4.2.

Table 4.2 - Statistic parameters for the period from the 20th to the 27th December 2010 in stationary mode. ($c=0.067\text{m}^2\text{s}^{-3}$)

$c(\text{m}^2\text{s}^{-3})$	Stationary Mode			
	0.067	With Currents (Simulation 11)	RMSE	
Hs(m)			Tm0,2(s)	Dir(°)
0.263			1.228	128.962
SI				
Hs			Tm0,2	Dir
0.227			0.261	---
ME				
Hs(m)		Tm0,2(s)	Dir(°)	
0.002		0.840	-47.137	
Without Currents (Simulation 12)		RMSE		
		Hs(m)	Tm0,2(s)	Dir(°)
		0.252	1.297	120.801
	SI			
	Hs	Tm0,2	Dir	
	0.218	0.276	---	
ME				
Hs(m)	Tm0,2(s)	Dir(°)		
-0.074	0.888	-58.284		

5 CONCLUDING REMARKS

This dissertation had as main objective the introduction of currents on the SWAN model simulations in the Diogo Lopes area, Brazil. The present work follows the previous studies by Ângelo (2012) and Matos (2013) with the aim of improving the calculated results with a special emphasis on the mean wave periods.

In what concerns the significant height the bottom friction coefficient is the key factor influencing the calculated values. Meanwhile, is possible to verify that better results are obtained when the bottom friction coefficient suggested by Bouws & Komen (1984) for wind sea is applied ($c = 0.067 \text{ m}^2\text{s}^{-3}$). As for the impact of the currents conditions in this wave parameter, is possible to say that its changes have almost no influence on the calculated significant wave heights. The stationary runs become more cost-effective in terms of the relation between the calculated values and computation time, since the non-stationary runs need more time to be accomplished and do not lead to better results.

Focusing on the mean periods and comparing with previous works in this very geographic location, we can observe a reasonable improvement on the obtained results, which previously were, in general, underestimated.

The analysis of the statistical parameters shows that improvements are achieved when a current field is present. The bottom friction coefficient which results on the better-calculated values is $c=0.067 \text{ m}^2\text{s}^{-3}$. However, a careful observation should be made concerning the 11th to the 12th of December period, where is possible to compare the results from two distinct geographic points inside de computational domain. The numerical simulations obtained for the $c=0.067 \text{ m}^2\text{s}^{-3}$ bottom friction coefficient, with the currents' field consideration were better for PT2 comparing with PT1.

6 REFERENCES

Ângelo, J. C. F. (2012). *Aplicação do modelo SWAN na caracterização da agitação marítima na zona adjacente ao estuário de Diogo Lopes , Brasil*. Instituto Superior Técnico.

- Booij, N., Ris, R., & Holthuijsen, L. (1999). A third-generation wave model for coastal regions. I- Model description and validation. *Journal of Geophysical Research*, 104(C4), 7649–7666.
- Bouws, E., & Komen, G. J. (1984). On the balance between growth and dissipation in a extreme, depth-limited wind-sea in the southern North Sea. *Journal of Physical Oceanography*, 13(9), 1653–1658.
- Hasselmann, K., Barnett, T. P., Bouws, E., Carlson, H., Cartwright, D. E., Enke, K., Ewing, J. A., Gienapp, H., Hasselmann, D. E., Kurseman, P., Meerburg, A., Müller, P., Olbers, D. J., Richter, K., Sell, W., Walden, H. (1973). Measurements of wind-wave growth and swell decay during the Joint North Sea Wave Project (JONSWAP) (Vol. 8). *Deutches Hydrographisches Institut*.
- Matos, M. de F. A. (2013). *Modelagem do clima de ondas e seus efeitos sobre as feições morfológicas costeiras no Litoral Setentrional do Rio Grande do Norte*. Universidade Federal do Rio Grande do Norte.
- Rosman, P. C. C. (2000). *Referência Técnica do SisBaHiA – SISTEMA BASE DE HIDRODINÂMICA AMBIENTAL*. Programa COPPE: Engenharia Oceânica, Área de Engenharia Costeira e Oceanográfica, Rio de Janeiro, Brasil.
- SWAN Team. (2008). *TECHNICAL DOCUMENTATION SWAN Cycle III version 40.51*.
- Tolman, H. L. (2002). *User manual and system documentation of WAVEWATCH-III version 2.22* (p. 133 pp.).
- U S Army Corps Of Engineers. (2002). *Coastal Engineering Manual. Coastal Engineering Manual*.
- Van der Westhuysen, A. J., Zijlema, M., & Battjes, J. a. (2007). Nonlinear saturation-based whitecapping dissipation in SWAN for deep and shallow water. *Coastal Engineering*, 54(2), 151–170.

7 ACKNOWLEDGEMENTS

To the Geoprocessing Laboratory from the Geology Department at Federal University of Rio Grande do Norte, for the bathymetry, wave parameters and tide data, and also to the Oceanic Engineering Program from COPPE/UFRJ for the *SISBAHIA* model operation.